Proceedings of the 4th Jagiellonian Symposium on Advances in Particle Physics and Medicine

Dose Distribution Comparison of Cerebrospinal Axis Irradiation. Helical Tomotherapy vs Proton Pencil Beam Scanning

A. Pędracka[a,b,*], B. Kiełtyka[a], K. Rawojć[a], Ł. Brandt[a], L. Mazur[c], T. Skóra[c], R. Kopeć[b], T. Kajdrowicz[b], E. Gora[c] and K. Kisielewicz[c]

[a] *University Hospital in Kraków, Jakubowskiego 2, 30-688 Kraków*
[b] *Institute of Nuclear Physics PAN, Radzikowskiego 152, 31-342 Kraków*
[c] *The Maria Sklodowska — Curie National Research Institute of Oncology in Krakow, Garncarska 11, 31-115 Kraków, Poland*

Doi: 10.12693/APhysPolA.142.408 *e-mail: apedracka@su.krakow.pl

Central nervous system tumors are diagnosed in 1–2% of all adult patients. Most cases are regarding brain tumors in which a standard of care is a combined treatment, i.e., surgical resection, radiotherapy, and chemotherapy. Radiation therapy in the cerebrospinal axis is becoming more common in oncological practice. The aim of this study is to compare dose distributions in treatment plans for the cerebrospinal axis adult patients irradiation using photon and proton beams. Six treatment cases were investigated. Dose distributions in the target and critical organs were analyzed in terms of uniformity, maximum, average, and minimum dose for target and integral dose. The high dose gradient areas that represent the resilience of treatment plans to uncertainties related to patient positioning and organ mobility were also investigated. The technique of proton radiotherapy requires joining the fields. The dose distributions obtained in proton plans are much more favorable in terms of the protection of critical organs and integral dose reduction. On the other hand, the treatment plans prepared for the photon helical technique are characterized by a greater dose distribution homogeneity in the areas where fields need to be joined in proton techniques. Those photon plans were proved to be less sensitive to errors resulting from the geometry of the patient's position. Irradiation times obtained for both techniques are not comparable. Each technique has its own benefits and, depending on availability, might be applied in the treatment of adult central nervous system tumors.

topics: helical tomotherapy (HT), radiotherapy (RT), proton pencil beam scanning (PBS), central nervous system (CNS) tumors

1. Introduction

Radiotherapy is a valuable treatment modality when radical surgery is hardly feasible due to difficult localization or the nature of the cancer type. Scalp irradiation is clinically used after surgical excision or as a primary treatment in conjunction with chemotherapy, depending on the extent of the disease [1]. To date, three-dimensional conformal radiotherapy (3D-CRT) has been the most clinically used for central nervous system (CNS) irradiation, although having certain limitations, i.e., problems related to multiple isocenters, need for junction movement during the treatment, or dose inhomogeneity at the beam junctions [1–3]. Moreover, large areas of organs at risk (OARs) localized in close proximity to the target can be irradiated due to the low conformity of 3D-CRT when compared to tomotherapy or other treatment modalities, i.e., proton beam.

These drawbacks of the 3D-CRT technique are highlighted by the fact that CNS is generally treated in paediatric patients, and they are known to have more severe side effects, such as endocrine and fertility dysfunction, growth and musculoskeletal abnormalities, neurobehavioural deficits, and secondary malignancies, due to unnecessary irradiation to OARs [2].

In recent years, methods of treating patients with ionizing radiation have been constantly developing, additionally achieving better and better clinical results [3, 4]. Several radiotherapy (RT) technologies have been developed, such as intensity modulated radiotherapy (IMRT), including helical tomotherapy (HT), volumetric modulated arc therapy, and particle beam therapy, to overcome the limitations of 3D-CRT and to make (RT) technique more feasible [3]. One of the most dynamically developing methods is helical tomotherapy (HT) [5–7]. Another highly specialized method of

radiotherapy that appears more and more frequently in clinical practice is RT based on the interaction of protons with matter, i.e., intensity modulated proton therapy (IMPT) [8, 9], which enables a high conformal dose distribution in the patient's body. In clinical practice, the most frequent techniques in external beam RT are related to dynamic techniques based on a standard medical accelerator.

HT combines highly precise rotational dose delivery with megavoltage computed tomography (MVCT). It provides a 6 MeV linear accelerator mounted on a gantry without a flattening filter (FFF) and an integrated detector for in-room image guidance with MVCT. While the gantry rotates continuously, the patient is translated through the gantry bore. The device is equipped with a binary multileaf collimator (MLC) consisting of 64 leaves to enable highly conformal dose delivery by dynamic field shaping. For the Radixact system with iDMS (Accuray, Sunnyvale, USA), the time for gantry rotation for MVCT acquisition has been adapted to 6 s. For dose delivery, dose rate of more than 1000 MU/min with a rotational speed of 1 to 5.08 rotations per minute was applied [10]. Recently, HT has been used to irradiate long and symmetrical types of structures, however, published clinical results are sparse [11, 12].

Proton beam irradiation (PBI) is another treatment mode, although less available in most countries. The main advantage of protons in radiotherapeutic applications over conventional radiation (photon and electron) is that the maximum dose (Bragg peak) occurs for protons at a certain depth, depending on the beam energy. The Bragg peak is a combination of increasing energy loss with decreasing proton energy and relatively slight beam scattering due to the large mass of the proton relative to the electron. Another advantage of the dose distribution for protons is the fact that the dose from the maximum falls very quickly to zero. The high dose gradient allows for the administration of the dose to neoplastic areas, avoiding excessive irradiation of the surrounding tissues, often including organs critical to the patient's health and life. Protons are accelerated in the cyclotron to an energy of 225 MeV (in this case), which corresponds with the range, R90 right, in water of 31.7 cm (PSTAR database). The range R90 right is defined as the depth at which the absorbed beam dose drops to 90% of its maximum value behind the Bragg Peak. Through a magnetic field, protons are formed into a narrow beam (pencil beam) and delivered with high accuracy to the tumor. In clinical use, the monoenergetic proton beam does not provide a uniform dose in the area of the entire neoplastic lesion [13]. Therefore the active beam delivery, where the treated volume is divided into layers achieved by protons with specific beam energy, was used.

The aim of this study is to compare dose distributions in treatment plans for the cerebrospinal axis adult patients irradiation using photon and proton beams.

2. Materials and methods

In this study, six treatment cases were analyzed. These were six adult male patients treated for germinoma, pineoblastoma, and medulloblastoma. The patients were qualified for proton beam radiotherapy and treated with a standard protocol. The helical tomotherapy plans were made in the treatment planning system additionally as a simulation.

All patients were immobilized using a thermoplastic mask in the head first supine position (HFS), then computed tomography (CT) scans were acquired with a 1.25 mm slice thickness. In both mentioned techniques, the same tomographic scans and contours of the critical organs and targets (RT structures) were used for treatment plan preparation. Target and OARs contouring were performed on the basis of clinical information, CTs, magnetic resonance imaging (MRI), and/or positron emission tomography (PET). The clinical target volume (CTV) in the analyzed cases was the cerebrospinal axis. The planning target volume (PTV) was defined as CTV plus a 0.5 cm margin. OARs included: optic nerves, eyes, lenses, thyroid, lungs, heart, liver, kidneys, and others not analyzed in this study. The treatment was prepared in a fractionation scheme of 1.8 Gy_{RBE}/fraction to 36 Gy_{RBE} of the total dose.

HT plans were generated using 6-MV X-ray beams of Radixact X9 (Accuray, Sunnyvale, USA). The Precision Treatment Planning System (Accuray, Sunnyvale, USA) was used with the superposition algorithm for plan calculation. Regarding the HT treatment conditions, a field width of 2.5 cm, a pitch of 0.420, and a modulation factor of 1.8 were used. The HT plans were not the real clinical plans used in treatment. Irradiation times for HT have been read in the treatment planning system.

In the case of proton RT planning, the Eclipse treatment planning system (TPS) (Varian Medical Systems, Palo Alto, USA) was used in intensity modulated proton therapy (IMPT) mode using a non-linear universal proton optimizer (NUPO) with robust optimization enabled. Optimization of robust was performed for 3.5% calibration curve uncertainty and 0.5 cm of isocenter shift for longitudinal direction, keeping the overlapping area safe from the potential shift. Shift isocenter was simulated by 0.5 cm in longitudinal one relative to the other, and the result we achieved was increasing the dose by 7%.

In all analyzed cases, the prepared treatment plans were based on combining 5 fields (3 separate isocenters). For the head area, a combination of 3 fields was used (90, 270, and 180 deg), and for the rest of the axis (spine), 2 posterior fields were used, overlapping. In the area of overlapping the fields,

TABLE I

Dose Constraints for PTV, CTV, and OARs. Abbreviations: PTV — planning target volume, CTV — clinical target volume, $D_{1\%,95\%}$ — dose to 1%, 95% volume of PTV/CTV/OAR, D_{av} — average dose, D_{max} — maximum dose, Vx – volume of the organ receiving $\geq$ x [Gy].

Structure	Criteria	Constraint
PTV	Mean dose	100%
	$D_{1\%}$	$< 107\%$
	$D_{95\%}$	$> 98\%$
CTV	Mean dose	$\geq 100\%$
	$D_{1\%}$	$< 107\%$
	$D_{95\%}$	100%
Retinas	D_{max}	45 Gy
Lens	D_{max}	< 6 Gy
Optical pathways	D_{max}	< 54 Gy
Thyroid	V30	$< 50\%$
Lung	D_{av}	< 13 Gy
	V20	$< 30\%$
Heart	D_{av}	< 26 Gy
	V30	$< 46\%$
Kidney	D_{av}	< 15 Gy
	V12	$< 5\%$
Liver	D_{av}	< 28 Gy

the method of optimizing the plans was focused on minimizing the maximum doses while maintaining the main criterion — all target volumes covered with 95% dose of the dose prescribe ($D_{95\%}$). During IMPT optimization, 0.5 cm fixed spot spacing was used to distribute the spots in the lateral direction and depth. A treatment machine was used with a 2.65 mm spot size (σ) (in air at the isocenter) of 225 MeV and a 6.6 mm spot size (σ) for minimum energy of 70 MeV. A spinal axis compensator was used instead of a range shifter to keep spot size as small as possible. All dose parameters are reported in Gy_{RBE}, assuming relative biological effectiveness (RBE) of 1.1 for protons.

A calculation grid of 2.0×2.0 mm^2 for all techniques was used. The plans have been optimized to cover the target in 95% of the volume with the given dose ($D_{95\%}$) and to ensure the most homogeneous dose distribution in the PTV volume. For all treatment modalities, after meeting the basic requirements for plan acceptability (Table I), the plans were optimized using the dose volume histogram (DVH) constraints to reduce the dose to the OARs to the lowest possible level. Constraints were specified by the authors.

Dose constraints used to prepare treatment plans for the studied group of patients are listed in Table I, however, plans were optimized to keep the doses for OARs as low as possible. Prioritization for RT structures was as follows: coverage of PTV and CTV, then limiting the doses for OARs.

3. Results

Dose distributions in the target were analyzed in terms of homogeneity index (HI), conformity index (CI), near maximum dose — here $D_{1\%}$ (dose to 1% volume of PTV), average dose, near minimum dose — here $D_{98\%}$ (dose to 98% volume of PTV), and others presented in Table II. For organs at risk, $D_{1\%}$, $D_{2\%}$ and average dose were analyzed and presented in Table III. Integral doses were also the subject of investigation. The high dose gradient areas that represent the resilience of treatment plans to uncertainties related to patient positioning and organ mobility were also analyzed. The technique of proton radiotherapy requires joining the fields. Field joints were subjected to deep analysis. The duration of treatment was also compared. Then the comparison of prepared plans was performed on RayStation, RaySearch Laboratories software.

An exemplary distribution of doses for both analyzed techniques is presented in Fig. 1. For IMPT plans in the area of field connection and for the area of the brain, there is a noticeable inhomogeneity in coverage with the given dose.

Additionally, for HT, the area beyond PTV in which the dose is deposited is larger (Fig. 1). It is worth noting that these are low doses dispersed over a large area, where, compared to the IMPT technique, the deposited doses may be nearly three times higher in a smaller volume. As the analysis of Table II shows, the obtained embraces for the target structures are comparable to each other.

TABLE II

Dose to PTV. Mean values with standard deviation for all six cases. Abbreviations: PTV — planning target volume, PBS — pencil beam scanning, HT — helical tomotherapy, $D_{1\%,2\%,50\%,95\%,98\%,99\%}$ — dose to 1%, 2%, 50%, 95%, 98%, 99% volume of PTV or OARs.

Parameter	Proton PBS	STD	HT	STD
PTV				
$D_{99\%}$	97.0%	0.4%	93.9%	1.9%
$D_{98\%}$	97.4%	0.4%	96.3%	0.8%
$D_{95\%}$	98.1%	0.2%	97.9%	0.1%
D_{av}	100.3%	0.2%	100.2%	0.3%
$D_{50\%}$	100.3%	0.2%	100.3%	0.3%
$D_{2\%}$	103.1%	0.5%	103.1%	0.7%
$D_{1\%}$	103.7%	0.5%	103.6%	0.7%
CTV				
$D_{99\%}$	97.3%	0.4%	97.7%	1.0%
$D_{98\%}$	97.7%	0.3%	98.4%	0.8%
$D_{95\%}$	98.3%	0.2%	99.0%	0.5%
D_{av}	100.2%	0.2%	100.5%	1.2%
$D_{50\%}$	100.2%	0.3%	100.5%	0.4%
$D_{2\%}$	102.8%	0.4%	102.8%	0.9%
$D_{1\%}$	103.3%	0.3%	103.6%	1.0%

TABLE III

Dose to OARs. Mean values with standard deviation for all six cases. Abbreviations: $D_{1\%,2\%}$ — dose to 1%, 2% volume of OARs, D_{av} — average dose, D_{pre} — dose prescribed.

Structure	Parameter	Proton PBS	STD	HT	STD
Eyes	$D_{1\%}/D_{pre}$	96.7%	4.8%	60.7%	5.1%
	$D_{2\%}/D_{pre}$	94.5%	5.9%	57.1%	5.3%
	D_{av}/D_{pre}	37.9%	9.9%	23.3%	2.9%
Lens	$D_{1\%}/D_{pre}$	12.3%	5.4%	11.1%	1.1%
	$D_{2\%}/D_{pre}$	11.7%	5.2%	10.9%	0.9%
	D_{av}/D_{pre}	7.1%	3.4%	9.6%	0.4%
Optic	$D_{1\%}/D_{pre}$	101.7%	2.7%	104.6%	1.5%
	$D_{2\%}/D_{pre}$	101.6%	2.6%	104.2%	1.6%
	D_{av}/D_{pre}	99.3%	1.8%	88.8%	5.0%
Thyroid	$D_{1\%}/D_{pre}$	14.8%	23.2%	25.6%	3.4%
	$D_{2\%}/D_{pre}$	12.3%	21.3%	24.9%	3.2%
	D_{av}/D_{pre}	1.76%	3.59%	19.0%	3.0%
Lung	$D_{1\%}/D_{pre}$	47.0%	21.1%	49.8%	13.7%
	$D_{2\%}/D_{pre}$	34.4%	18.0%	45.1%	12.2%
	D_{av}/D_{pre}	2.04%	1.13%	19.9%	3.8%
Kidney	$D_{1\%}/D_{pre}$	14.9%	13.5%	35.0%	5.4%
	$D_{2\%}/D_{pre}$	8.39%	8.16%	33.5%	5.2%
	D_{av}/D_{pre}	0.54%	0.50%	19.9%	2.3%
Heart	$D_{1\%}/D_{pre}$	0.30%	0.58%	31.2%	1.3%
	$D_{2\%}/D_{pre}$	0.07%	0.14%	29.9%	1.3%
	D_{av}/D_{pre}	0.01%	0.03%	18.3%	1.1%
Liver	$D_{1\%}/D_{pre}$	1.01%	1.75%	33.0%	3.5%
	$D_{2\%}/D_{pre}$	0.12%	0.15%	31.3%	3.4%
	D_{av}/D_{pre}	0.08%	0.11%	16.7%	0.9%

As shown in Table I, the assumed criteria for the preparation of plans were met for both target volumes in each of the analyzed plans.

Homogeneity index (HI) was calculated for both target volumes, i.e., PTV and CTV, with the formula [14]

$$\mathrm{HI} = \frac{\mathrm{D}_{2\%} - \mathrm{D}_{98\%}}{\mathrm{D}_{\mathrm{pre}}} \times 100, \tag{1}$$

where D_{pre} is dose prescribed in $\mathrm{Gy}_{\mathrm{RBE}}$.

The obtained results (average of 6 cases) are very similar in terms of the compared techniques. The results for PTV are 6.84 ± 1.15 and 5.75 ± 0.75 for techniques HT and pencil beam scanning (PBS), respectively. For CTV they are 5.00 ± 1.11 and 5.05 ± 0.61, respectively. This indicates obtaining plans of comparable homogeneity by virtue of the techniques with little indication of PBS for PTV and HT for CTV.

Conformity index (CI) was determined in accordance with the equation

$$\mathrm{CI} = \frac{\mathrm{V}_{\mathrm{REF}}}{\mathrm{V}_{\mathrm{PTV}}}, \tag{2}$$

where $\mathrm{V}_{\mathrm{REF}}$ is the reference isodose volume — here 95%, and $\mathrm{V}_{\mathrm{PTV}}$ is the volume of PTV structure.

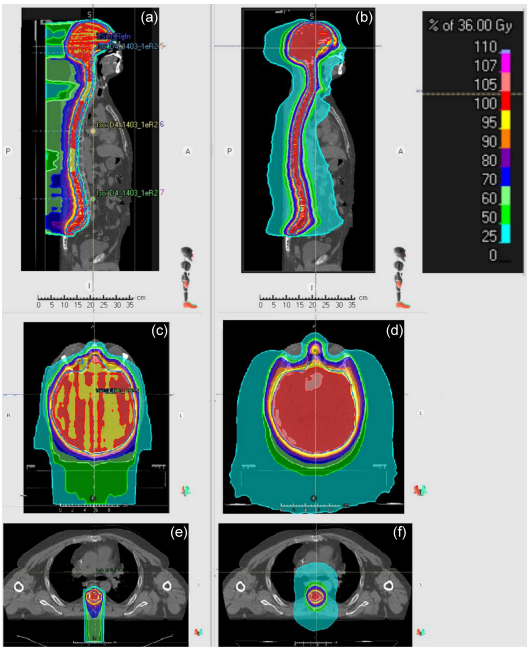

Fig. 1. Example of dose distribution using proton PBS (a, c, e) and helical tomotherapy (b, d, f) for one case. Sagittal section (a, b) and two horizontal section: head (c, d) and lungs (e, f).

CI (average of 6 cases) for PBS is 1.25 ± 0.04 instead 1.48 ± 0.15 for HT, so the obtained values clearly indicate a better dose distribution in the PBS technique.

Dose-volume histograms (DVH) are shown in Fig. 2 for selected OARs and PTV. From the analysis of the histograms, it can be clearly seen that all structures located more than a few centimeters from the target's volume achieve much lower doses in the plans prepared in the PBS technique compared to HT. There is also a noticeable tendency that with the reduction of the OAR and target volume (TV) distance, both the average dose and the maximum dose clearly increase for the proton technique. In single structures (e.g., optic nerves or retinas), there is a noticeable tendency to obtain worse dose distributions compared to tomotherapy.

Due to the specificity of the irradiated area for the eyes and optic nerves, we observe high point and medium doses. This is due to their partial inclusion in PTV.

In the case of HT, apart from the above-mentioned case, there is a clear tendency to distribute the dose throughout the body. This can be seen from the comparison of the average dose and the maximum dose. For HT, the D_1/D_{av} ratios are in the range of 1.5–3, while for PBS, the ratio is much higher, i.e., even up to 30.

The integral dose value — the quantity representing the amount of energy deposited in the whole patient's volume, is 2.7 times higher for HT ($25.8 \pm 2.9\%$ of the prescribed dose) than for PBS ($9.7 \pm 1.3\%$ of the prescribed dose).

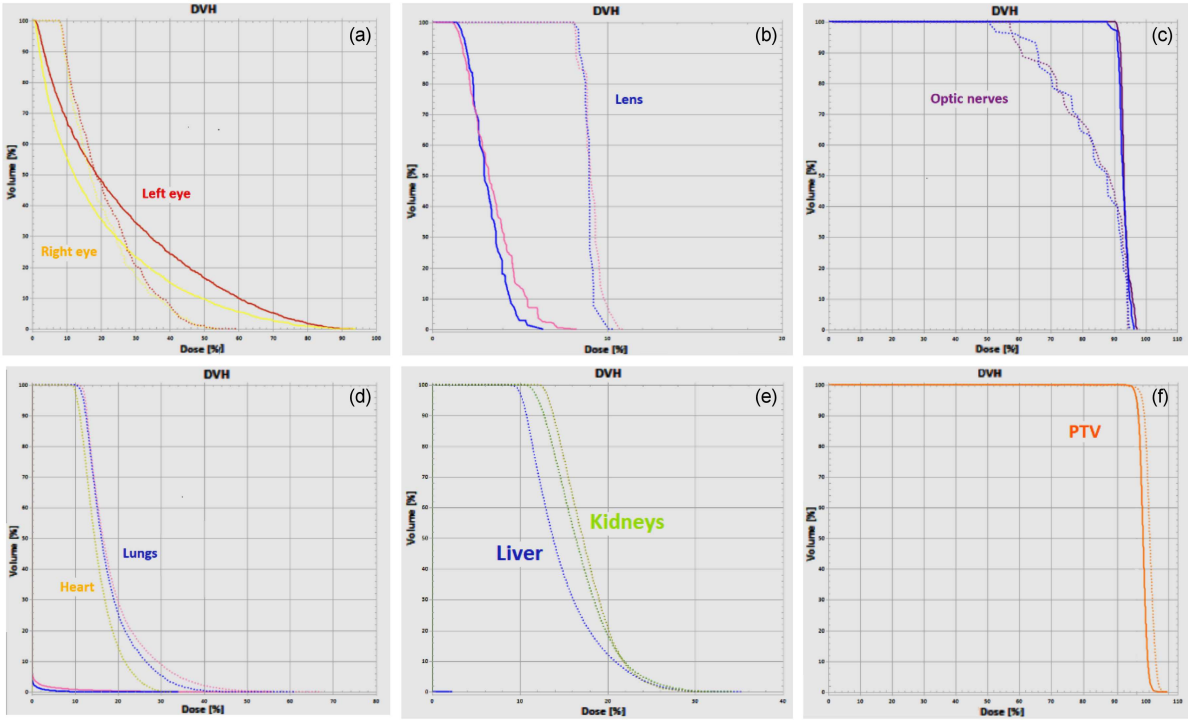

Fig. 2. Example of dose-volume histogram (DVH) for the case from Fig. 1. The solid line shows the results obtained for irradiation with the PBS technique, while the dashed line shows the results for HT.

The treatment plans prepared for the photon helical technique are characterized by a greater dose distribution homogeneity in the areas where fields had to be joined in proton techniques. Those photon plans were proved to be less sensitive to errors resulting from the geometry of the patient's position. Additionally, in order to be able to better define the patient's exposure, the low distributions of 5% and 10% isodoses were compared. The size of the area covered by isodose in the HT plan compared to the PBS plans is 7.1 ± 0.5 and 11.1 ± 1.2 times greater for 5% and 10%, respectively.

The duration of the therapeutic session for HT is about $\frac{1}{3}$ shorter, compared to PBS, due to the specificity of the dose delivery, including the lack of several isocenters for HT, which is also related to the necessity to perform multiple verifications of patient's position imaging for PBS.

4. Conclusions

The advantages of proton radiation make it possible to reduce the probability of complications after irradiation while maintaining a low degree of complications, and to increase the dose within the tumor and thus increase the probability of its destruction. Maximum tumor control probability (TCP) can be achieved with minimum normal tissue complication probability (NTCP), reducing the risk of secondary cancer induction. The dose distributions obtained in proton plans are much more favorable in terms of the protection of critical organs and the integral dose reduction — which is very important in the case of pediatric patients — reducing the risk of secondary cancer induction. However, the uncertainty of dose delivery to the irradiated volume is lower in helical tomotherapy.

On the other hand, the treatment plans prepared for the photon helical technique are characterized by a greater dose distribution homogeneity in the areas where fields needed to be joined in proton techniques. Those photon plans were proved to be less sensitive to errors resulting from the geometry of the patient's position. Due to simultaneous dose delivery in HT, there is are field junctions that may provide hot spots in junction regions. Irradiation times obtained for both techniques are not comparable, being $\frac{1}{3}$ shorter for HT.

Each technique has its own benefits and, depending on availability, might be applied in the treatment of adult CNS malignant tumors.

References

[1] F. Cuccia, V. Figlia, A. Palmeri, et al. *Rare tumors* **9**, 6942 (2017).

[2] P. Borghetti, S. Pedretti, L. Spiazzi et al., *Radiat. Oncol.* **11**, 59 (2016).

[3] G. Peng, T. Wang, K.Y. Yang, S. Zhang, T. Zhang, Q. Li, J. Han, G. Wu, *Radiother. Oncol.* **104**, 286 (2012).

[4] N. Tomita, N. Soga, Y. Ogura, J. Furusawa, H. Tanaka, Y. Koide, H. Tachibana, T. Kodira, *Asia. Pac. J. Clin. Oncol.* **15**, 18 (2019).

[5] C. Leitzen, T. Wilhelm-Buchstab, S. Stumpf et al., *Strahlenther Onkol.* **195**, 668 (2019).

[6] N. Tomita, T. Kodaira, H. Tachibana, T. Nakamura, R. Nakahara, H. Inokuchi, N. Mizoguchi, A. Takada, *Br. J. Radiol.* **82**, 756 (2009).

[7] K. Otto, *Med. Phys.* **35**, 310 (2008).

[8] D. Schulz-Ertner, H.J. Tsujii, *Clin. Oncol.* **25**, 953 (2007).

[9] M. Steneker, A. Lomax, U. Schneider, *Radiother. Oncol.* **80**, 263 (2006).

[10] K.M. Kraus, S. Kampfer, J.J. Wilkens, L. Schüttrumpf, S.E. Combs *Sci. Rep.* **10**, 4928 (2020).

[11] O. Jäkel, *Radiat. Prot. Dosim.* **137**, 156 (2009).

[12] J. Lee, E. Kim, N. Kim, H.K. Byun, C.-O. Suh, Y. Chung, H.I. Yoon, *Sci. Rep.* **11**, 6120 (2021).

[13] T. Mizuno, N. Tomita, T. Takaoka, M. Tomida, H. Fukuma, T. Tsuchiya, Y. Shibamoto, *Technol. Cancer Res. Treat.* **20**, 1533033820985866 (2021).

[14] K. Tejinder, S. Kuldeep, S. Vikraman, K.P. Karrthick, S. Shyam Bisht, *J. Med. Phys.* **37**, 207 (2012).